RESEARCH ARTICLE | OCTOBER 21 2024

Application of conductive graphene films for high-performance hemispherical resonator gyroscopes

Fei Wang; Jian Wang; Zhuqing Yi ; Chuanren Ye ; Yanwu Zhu

Appl. Phys. Lett. 125, 174102 (2024)
https://doi.org/10.1063/5.0230846

Applied Physics Letters ARTICLE pubs.aip.org/aip/apl

Application of conductive graphene films for high-performance hemispherical resonator gyroscopes

Cite as: Appl. Phys. Lett. **125**, 174102 (2024); doi: 10.1063/5.0230846
Submitted: 26 July 2024 · Accepted: 10 October 2024 ·
Published Online: 21 October 2024

Fei Wang,[1,2] Jian Wang,[2] Zhuqing Yi,[2] Chuanren Ye,[1] and Yanwu Zhu[1,3,a)]

AFFILIATIONS

[1]Department of Materials Science and Engineering, School of Chemistry and Materials Science, University of Science and Technology of China, Hefei, Anhui 230026, China
[2]Hunan 208 Advanced Technology Company Limited, Changsha, Hunan 410205, China
[3]Hefei National Research Center for Physical Sciences at the Microscale & Key Laboratory of Precision and Intelligent Chemistry, University of Science and Technology of China, Hefei, Anhui 230026, China

[a)]**Author to whom correspondence should be addressed:** zhuyanwu@ustc.edu.cn

ABSTRACT

Hemispherical resonator gyroscope is a type of solid-state gyroscope, in which the fused silica hemispherical resonator with a high-quality factor (Q factor) is the key for the fabrication of high-performance devices. However, the metal film coated on the silica as the electrode for trigging the resonance often leads to the largely deteriorated Q factor. In this work, high-quality graphene films with controllable number of layers are uniformly coated on silica utilizing C_2H_4 as precursor in chemical vapor deposition. Replacing the metal film as the electrode, the hemispherical resonator coated with graphene demonstrates a Q factor of 3.38×10^6, with a high retention of 77.17%. At an optimized preparation temperature of 1130 °C, the graphene film shows a good adhesion with the silica hemisphere, providing an excellent candidate as the electrode for high-performance hemispherical resonators.

The hemispherical resonator gyroscope (HRG) has been used in inertial navigation systems, precision pointing, deep space exploration, and other fields because of high precision, long lifetime, and potential in miniaturization of HRG devices.[1–4] A classic HRG device as shown in Fig. 1(a) is composed of an excitation shell, a hemispherical resonator, and a detection base, in which the hemispherical resonator is the key component, required to own an excellent symmetry for low energy dissipation and low frequency split in the vibrating mode, which are key merits for a high-quality factor (Q factor) of HRG.[5] Typically, the fused silica coated with metal is used as the resonator, working as a medium of resonant standing wave with two wineglass modes and four nodes.[6] Due to the residual stress and unsatisfactory adhesion of the deposited metal, however, the Q factor of the hemisphere coated with metal is often reduced to less than 40% of that before coating. To minimize the influence of the metal coating, methods such as matching the coefficient of thermal expansion (CTE) or post thermal treatment have been developed. For example, an extremely thin chromium (Cr) intermediate layer with a CTE = 4.9 ppm K^{-1} was added between the fused silica (CTE = 0.5 ppm K^{-1}) and the functional gold (Au) (CTE = 14.2 ppm K^{-1}) coating for the better adhesion.[7] The Q factor of the hemispherical resonator was reduced by 55%–60% after coating 20 nm Cr/Au layer.[8] On the other hand, Chen *et al.* found that the uniformity of the coating thickness on hemisphere affects the accuracy of the gyroscope, by analyzing the dynamic equation of hemispherical resonator.[9] Other factors such as the intrinsic modulus and the residual stress in the metal film also influence the vibration performance of the hemispherical resonator by greatly decreasing the Q value of the hemispherical resonator.[8] Since these drawbacks are related to the intrinsic feature of the metal coating, candidates with satisfactory electric conductivity and adhesion are needed to improve the Q factor of the hemispherical resonator.

With an electric conductivity of above 10^6 S m^{-1},[10] a thermal conductivity of up to 5300 W m^{-1} K^{-1},[11] and Young's modulus of 1 TPa,[12] graphene is potentially an excellent replacement of metal films as the electrode for high-performance hemispherical resonators. Especially, the low density (0.77 mg m^{-2}) and the high stiffness (42 N m^{-1}) may alleviate the influence of electrode on the fused silica once the electric conductivity and interface adhesion with silica meet

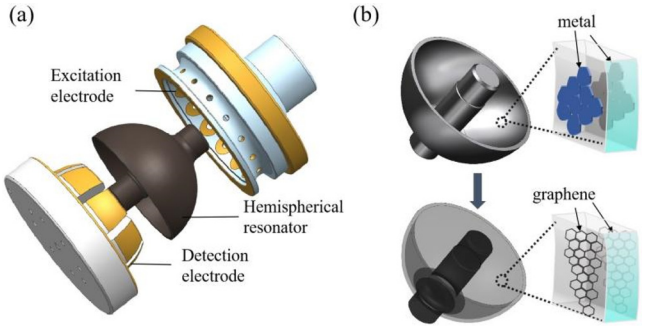

FIG. 1. (a) Structure of HRG including three main components (outer base, the resonator, and inner base). (b) Schematic showing the replacement of metal coating by graphene.

the requirement in devices.[13] Furthermore, graphene can be prepared by chemical vapor deposition (CVD), providing high-quality, large-area, and reasonable controllability of the number of layers.[14–16] It was reported that graphene grown on glass substrate has a conductivity of 0.55 kΩ sq^{-1}, by employing a metal-capping-assisted transfer-free method.[17] To ensure that the hemispherical resonator is not polluted by metal catalyst, it is necessary to develop the graphene growth by catalyst-free CVD directly on silica. So far, graphene has not been prepared on the hemispherical silica and the feasibility of graphene as the electrode for triggering the resonator remains to be explored.

In this work, we carry out the growth of graphene by CVD on the hemispherical silica resonator. Since the hemispherical shape interferes the flow of carrier gas, thus the nucleation of graphene on silica, an atmospheric pressure CVD (APCVD) is used.[18–21] The experimental conditions using C_2H_4 as carbon precursor have been investigated for a graphene coverage of 100% on the hemispherical resonator uniformly. An optimized deposition carried out at 1130 °C for 3–4 h results in a resistivity of 1.62 kΩ cm^{-1} on the resonator. The Q factor retention of the hemispherical resonator is 77.17%, validating the feasibility of using graphene as the conductive film of HRG.

Figure 1 schematically shows the structure of HRG and the replacement of metal electrode by graphene. Here, HRG works with the force-to-rebalance mode, in which the hemisphere resonator is excited by 16 excitation electrodes, and the detection base consisting of eight detection electrodes is used to collect the signal. The bare hemispherical resonator made with computer numerical control (CNC) using fused silica as the raw material has a complex architecture and abundant micro-curvatures. During the preparation especially in the grinding and polishing machining, the surface damage is inevitably introduced. Thus, a cleaning process has been executed in concentrated sulfuric acid for 2 h to eliminate the detrimental influence from surface damage. After that the resonator was soaked again in diluted hydrochloric acid (20 vol. %) for 2 h and finally rinsed with de-ionized water before drying. The hemispherical resonator was then heated in a flowing Ar/H_2 in a horizontal tube furnace at a heating rate of 2.5 °C min^{-1}. Then, the graphene film was prepared by heating the hemispherical resonator at 1130 °C for 3–4 h in Ar/H_2/C_2H_4 (flow rate: 100/50/0.8 sccm). Raman spectra were collected with Renishaw in Via Raman Microscope (UK). Scanning electron microscopy (SEM) images were obtained with a field-emission SEM (Hitachi SU8220, Japan) and the vibration information obtained with a scanning laser vibrometer (Polytech PSV-500, Germany).

Figure 2(a) shows a hemispherical resonator before deposition of graphene, which shows a translucent feature due to the rough surface. After the deposition of graphene at 1130 °C for 3.5 h, Fig. 2(b) shows that the inner and outer surfaces of the resonator are covered by a uniform black layer, and the resonator maintains the intact shape. The SEM image in Fig. 2(c) shows the morphology of the graphene deposited on the quartz substrate under the same conditions for the convenience of characterizations. From SEM, we can see that the film consists of ad-layers with a lateral size of ∼5.0 μm on the continuous first-layer deposition. Figure 2(d) shows the Raman spectra of the film deposited on the quartz substrates with different experimental conditions, from which three notable bands, i.e., the disorder-induced D band located at 1346 cm^{-1}, G band at 1599 cm^{-1} caused by in-plane vibration of sp^2 carbon, and the second-order harmonic 2D band at 2690 cm^{-1}, are determined, indicating the preparation of graphene.[22] The intensity ratio of 2D band to G band, I_{2D}/I_G, is around 1.0 for all three samples, similar to 2–3 layers of graphene made by CVD on metals.[23,24] Defects in graphene prepared by CVD without metallic catalyst are common, so I_D/I_G needs to be optimized for the low content of defects and a high electric conductance.[25] For the deposition duration of 4, 3.5, or 3.25 h, the corresponding I_D/I_G value is 0.45, 0.44, or 0.94, respectively, indicating that the graphene prepared at 1130 °C and 3.5 h has a relatively low defect density. To further verify the adhesion between graphene and the hemispherical resonator, the resonator after graphene coating was ultrasonically treated for 2 h at a power of 200 W (operated at 53 kHz) and then subjected to Raman spectroscopy. The comparison of 2D peak intensity mapping, as shown in Figs. 2(e) and 2(f), indicates that the graphene layer remains on the surface of resonator with the similarly distributed density of 2D peak. That is, the adhesion of graphene on the resonator is high enough to resist the ultrasonic treatment.

The Q factor of hemispherical resonators was obtained in a vibration measurement system working at a pressure lower than 5×10^{-3} Pa, as shown in Fig. 3(a). The vibration is excited by a piezoelectric (PZT), and a scanning laser vibrometer (SLV) is used for detection. The sweeping frequency is applied to the hemispherical resonator by PZT, and the vibration signal along the lip of the resonator is obtained by SLV. The intrinsic frequency of the resonator is obtained after fast Fourier transformation (FFT) of the signal. The amplitude ringdown time was measured by exciting the wineglass mode at its resonant frequency followed by abruptly turning off the excitation signal. The time decay from the initial amplitude of the vibration to 1/e is used to calculate the Q factor of n = 2 wineglass mode. Figure 3(b) shows the Q factors of the resonators before and after graphene coating performed at 1130 °C with different deposition time. The Q factor of the original resonators falls in 4.38–4.71 × 10^6, which decreases to 2.93–3.38 × 10^6 after coating with graphene. The highest Q factor retention is 77.17%, obtained from the growth time of 3.5 h (compared to 69.17% for 3.25 h or 62.21% for 4 h). Figure 3(c) shows that the film thickness of ∼6, ∼10, or ∼14 nm for the deposition duration of 3.25 h, 3.5 h, or 4 h, respectively, was obtained by tapping mode AFM measurement (Bruker ICON2). Based on the single layer thickness of 0.8–1.5 nm,[26,27] for graphene films prepared without metal catalyst,[28,29] the AFM measurement gives an estimated layer number of 6–10 for the deposition duration of 3.5 h. With the increase in the thickness, the

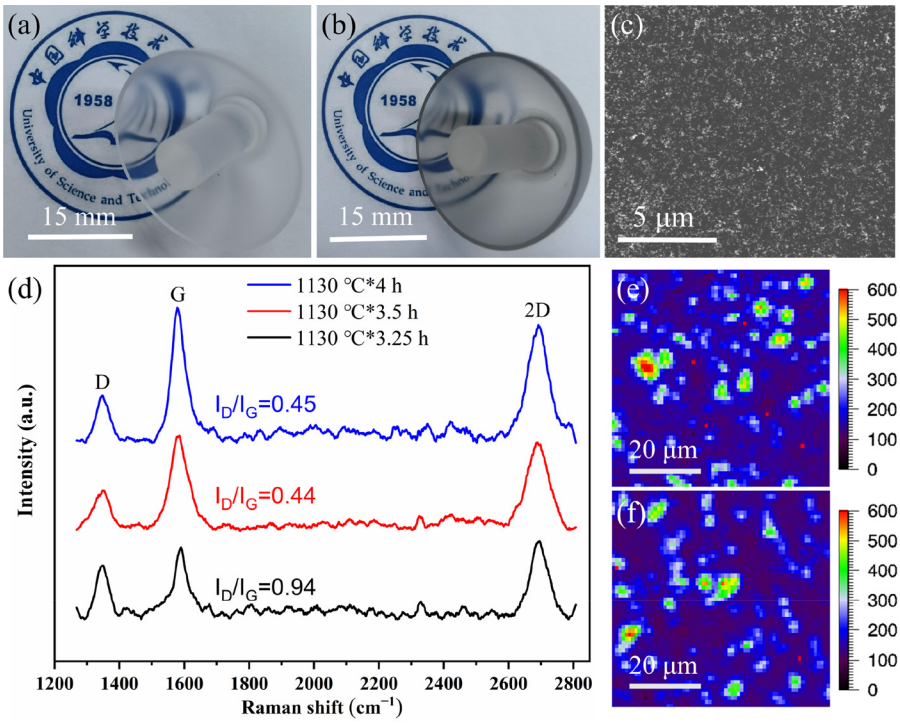

FIG. 2. A hemispherical resonator (a) before and (b) after graphene coating. Typical (c) SEM image and (d) Raman spectra of graphene with different experimental conditions. Raman Mapping of 2D peak intensity (e) before and (f) after sonicating the resonator coated with graphene.

resistivity of graphene reduces from 1.98 to 1.62 kΩ cm^{-1}. Different from the higher-quality deposition on metals such as Cu, the direct deposition of graphene on silica may be accompanied by the uncomplete coverage and the deposition of amorphous carbon, which would also explain the difference in layer number obtained from Raman and AFM. When the deposition time increases from 3.25 to 3.5 h, the more coverage of graphene leads to the lower value of I_D/I_G,[29,30] but the deposition of amorphous carbon could neutralize the I_D/I_G value for

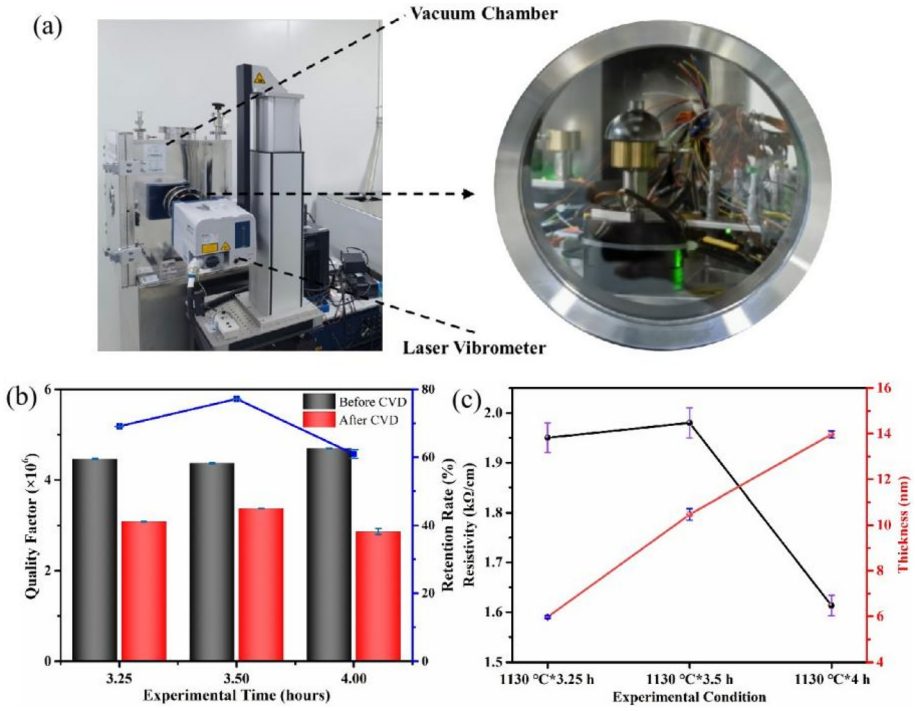

FIG. 3. (a) System for the measurement of vibration parameters showing the hemispherical resonator in the vacuum chamber. (b) Q factors and retention of the resonators before and after graphene coating. (c) Electric resistivity and thickness of graphene films.

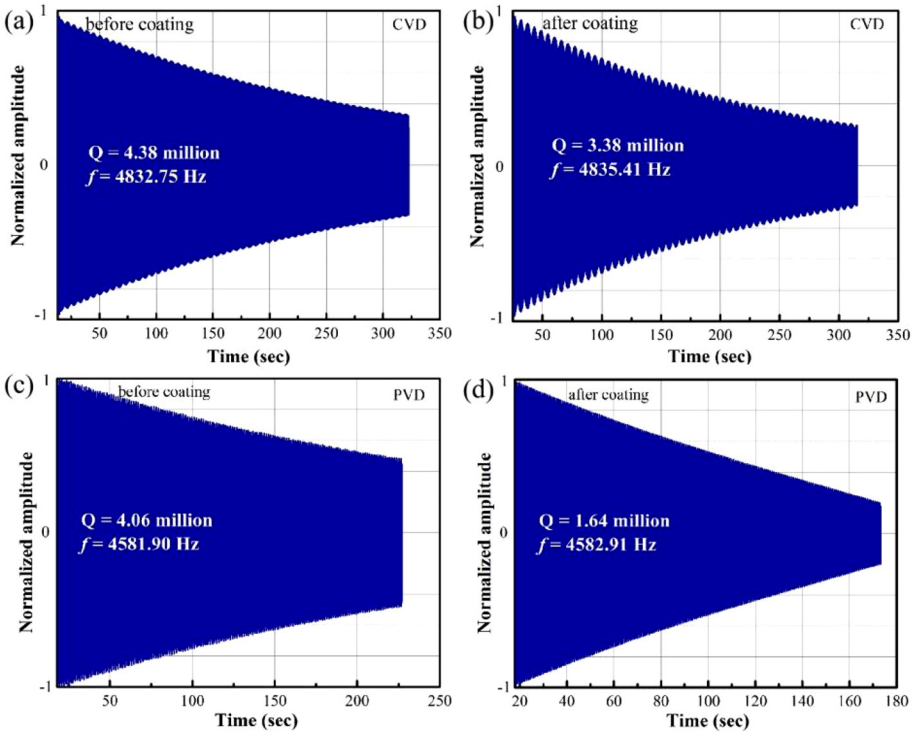

FIG. 4. Resonance curves of the hemispherical resonator (a) before and (b) after coating with graphene. Resonance curves of the hemispherical resonator (c) before and (d) after coating with Cu/Ni film.

the deposition duration of 4 h.[31,32] Combining all these facts, we think that the deposition duration of 3.5 h is a proper balance between the coverage and deposition of amorphous carbon in our preparation conditions for the better Q factor retention.

Now, we compare the performance of a hemispherical resonator coated with graphene (1130 °C, 3.5 h) with another resonator coated with Cu/Ni ($wt/wt = 1{:}1$) with a thickness of ~10 nm by physical vapor deposition (PVD). From the resonance curves shown in Fig. 4(a), we can see the Q factor of the bare resonator is 4.38×10^6 at n = 2 wineglass mode. Figure 4(b) shows the Q factor of the hemispherical resonator after coating with graphene is reduced to 3.38×10^6, with a retention of 77.17%. In the resonance frequency, the resonator is increased by 2.66 Hz after coating with graphene, probably due to the heat treatment and the increased thickness of the hemispherical resonator.[33,34] In contrast, Figs. 4(c) and 4(d) show that the Q factors of the resonator are dramatically reduced to 1.64×10^6 after Cu/Ni coating from the original 4.06×10^6, corresponding to a retention of 40%. The low retention for metal coating may be attributed to the uneven and residual stress in the metal film prepared by magnetron sputtering, which, however, is much alleviated in the graphene film due to the more uniform and less residual stress.

To further verify the practical performance of the graphene film, printed circuit board (PCB) was used to electrically excite a hemispherical resonator coated with graphene prepared at 1130 °C for 3.5 h. Figure 5(a) shows the field diagram of hemispherical resonator excited by PCB, which is applied by the capacitor between the electrode on the PCB and the lip edge of the hemispherical resonator. The alternating current voltage applied to a certain electrode of the PCB has the same frequency as the hemispherical resonator n = 2 wineglass mode. The resonance curve detected by SLV is shown in Fig. 5(b), from which a Q factor of 3.50×10^6 is obtained, slightly larger than the Q factor obtained by PZT excitation (3.38×10^6). The difference may be caused by the different excitation modes, as PZT is excited through the center rod of the hemispherical resonator, which could lead to a larger loss. The actual use scenarios by PCB electrical excitation further indicate that the graphene film instead of the metal film at the electrode of hemispherical resonator is feasible.

In summary, graphene films with satisfactory electrical conductivity have been fabricated on hemispherical resonators by catalyst-free CVD. The suitable experimental condition has been optimized as a growth temperature of 1130 °C for 3.5 h. The maximum Q factor of 3.38×10^6 with the highest retention rate of 77.17% is obtained, based on a resistivity of 1.98 kΩ cm^{-1} for the graphene film. Such a

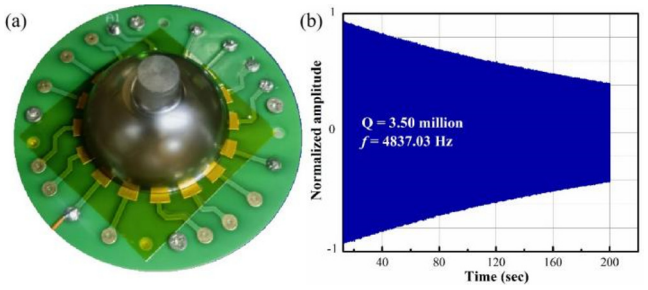

FIG. 5. (a) Field diagram of hemispherical resonator excited by PCB. (b) Resonance curve of the resonator after coating at the temperature of 1130 °C for 3.5 h, which excited by PCB.

performance is higher than the situation for the Cu/Ni coating with the similar thickness, where a Q factor retention of 40.39% is obtained. With good uniformity and adhesion, graphene has shown a great potential as a replacement of metal coating on the hemispherical resonator, for the higher Q factor retention, thus better comprehensive performance.

This work was supported by the National Key R&D Program of China (Grant No. 2020YFA0711502), the Natural Science Foundation of China (Nos. 52325202 and 52273239), and the Key R&D Program of Jiangsu Province under Grant No. BE2021007-1.

AUTHOR DECLARATIONS

Conflict of Interest

The authors have no conflicts to disclose.

Author Contributions

Fei Wang: Conceptualization (lead); Data curation (equal); Investigation (lead); Writing – original draft (lead). **Jian Wang:** Data curation (equal); Investigation (equal); Writing – original draft (equal). **Zhuqing Yi:** Data curation (equal); Writing – review & editing (equal). **Chuanren Ye:** Data curation (equal). **Yanwu Zhu:** Conceptualization (lead); Funding acquisition (lead); Investigation (equal); Writing – review & editing (lead).

DATA AVAILABILITY

The data that support the findings of this study are available from the corresponding author upon reasonable request.

REFERENCES

[1]F. Delhaye and J. P. Girault, in 25th Saint Petersburg International Conference on Integrated Navigation Systems (2018).
[2]A. Vafanejad and E. Sok Kim, in 18th International Conference on Solid-State Sensors, Actuators and Microsystems (2015).
[3]D. M. Rozelle, in 19th AAS/AIAA Space Flight Mechanics Meeting (2009).
[4]S. Askari, M. H. Asadian, and A. M. Shkel, in IEEE International Symposium on Inertial Sensors and Systems (2018).
[5]Z. Y. Xu, G. X. Yi, M. J. Er, and C. Huang, Sensors **19**(6), 1291 (2019).
[6]C. Li, Y. C. Wang, C. K. Ahn, C. X. Zhang, and B. Wang, IEEE Trans. Ind. Electron. **70**(6), 6425 (2023).
[7]Y. S. Wang, Y. W. Lin, J. Glaze, G. D. Vukasin, D. D. Shin, H. K. Kwon, D. B. Heinz, Y. H. Chen, D. D. Gerrard, and T. W. Kenny, J. Microelectromech. Syst. **30**(2), 193 (2021).
[8]D. M. Wang, M. H. Asadian, W. Guan, D. Hii, A. R. Parrish, and A. M. Shkel, J. Microelectromech. Syst. **31**(6), 877 (2022).
[9]X. Chen, S. Q. Ren, H. B. Zhao, and J. Y. Qi, Aerosp. Control and Appl. **35**(3), 29 (2009).
[10]K. S. Novoselov, A. K. Geim, S. V. Morozov, D. Jiang, Y. S. Zhang, S. V. Dubonos, I. V. Grigorieva, and A. A. Firsov, Science **306**(5696), 666 (2004).
[11]J. H. Seol, I. Jo, A. L. Moore, L. Lindsay, Z. H. Aitken, M. T. Pettes, X. S. Li, Z. Yao, R. Huang, and D. Broido, Science **328**(5975), 213 (2010).
[12]X. J. Tan, J. Wu, K. W. Zhang, X. Y. Peng, L. Z. Sun, and J. X. Zhong, Appl. Phys. Lett. **102**(7), 071908 (2013).
[13]C. G. Lee, X. D. Wei, J. W. Kysar, and J. Hone, Science **321**(5887), 385 (2008).
[14]J. B. Wang, Z. Ren, Y. Hou, X. L. Yan, P. Z. Liu, H. Zhang, H. X. Zhang, and J. J. Guo, New Carbon Mater. **35**(3), 193 (2020).
[15]T. Kato and R. Hatakeyama, ACS Nano **6**(10), 8508 (2012).
[16]J. Y. Sun, Y. B. Chen, M. K. Priydarshi, T. Gao, X. J. Song, Y. F. Zhang, and Z. F. Liu, Adv. Mater. **28**(46), 10333 (2016).
[17]Q. Q. Zhuo, Q. Wang, Y. P. Zhang, D. Zhang, Q. L. Li, C. H. Gao, Y. Q. Sun, L. Ding, Q. J. Sun, and S. D. Wang, ACS Nano **9**(1), 594 (2015).
[18]J. Y. Chen, Y. G. Wen, Y. L. Guo, B. Wu, L. P. Huang, Y. Z. Xue, D. C. Geng, D. Wang, G. Yu, and Y. Q. Liu, J. Am. Chem. Soc. **133**(44), 17548 (2011).
[19]J. Hwang, M. Kim, D. Campbell, H. A. Alsalman, J. Y. Kwak, S. Shivaraman, A. R. Woll, A. K. Singh, R. G. Hennig, and S. Gorantla, ACS Nano **7**(1), 385 (2013).
[20]J. Y. Chen, Y. L. Guo, L. L. Jiang, Z. P. Xu, L. P. Huang, Y. Z. Xue, D. C. Geng, B. Wu, W. P. Hu, and G. Yu, Adv. Mater. **26**(9), 1348 (2014).
[21]D. C. Wei, Y. H. Lu, C. Han, T. C. Niu, W. Chen, and A. T. Wee, Angew. Chem., Int. Ed. **52**(52), 14121–14126 (2013).
[22]O. Yoshito, S. Vantasin, I. S. Yang, J. Son, J. Hong, Y. Y. Tanaka, Y. Nakata, Y. Ozaki, and N. Naka, Appl. Phys. Lett. **108**(16), 163110 (2016).
[23]C. X. Deng, W. W. Lin, S. Eimer, D. Ravelosona, C. Chappert, and W. S. Zhao, in 13th IEEE International Conference on Nanotechnology (2013).
[24]M. Irannejad, W. Alyalak, S. Burzhuev, A. Brzezinski, M. Yavuz, and B. Cui, Trans. Electr. Electron. Mater. **16**(4), 169 (2015).
[25]B. Y. Ju, W. S. Yang, Q. Zhang, M. Hussain, Z. Y. Xiu, J. Qiao, and G. H. Wu, Int. J. Miner. Metall. Mater. **27**, 1179 (2020).
[26]C. Backes, T. M. Higgins, A. Kelly, C. Boland, A. Harvey, D. Hanlon, and J. N. Coleman, Chem. Mater. **29**(1), 243 (2017).
[27]W. Liu, Z. D. Chen, Z. Zhang, P. X. Jiang, Y. G. Chen, E. Paek, Y. X. Wang, and D. Mitlin, Energy Environ. Sci. **14**(1), 382 (2021).
[28]Z. Chen, Y. Qi, X. Chen, Y. Zhang, and Z. Liu, Adv. Mater. **31**(9), 1803639 (2019).
[29]M. Li, P. Zou, Z. Chen, R. Zhao, C. Tang, S. Wang, Y. Ma, and L. Ma, ACS Appl. Nano Mater. **6**(12), 10817–10825 (2023).
[30]H. Ci, J. Chen, H. Ma, X. Sun, X. Jiang, K. Liu, J. Shan, X. Lian, B. Jiang, R. Liu, B. Liu, G. Yang, W. Yin, W. Zhao, L. Huang, T. Gao, J. Sun, and Z. Liu, Adv. Mater. **34**(51), 2206389 (2022).
[31]J. Kotakoski, A. V. Krasheninnikov, U. Kaiser, and J. C. Meyer, Phys. Rev. Lett. **106**(10), 105505 (2011).
[32]J. H. Lee, Y. S. Song, and E. Lim, Appl. Phys. Lett. **110**(14), 143104 (2017).
[33]Y. M. Luo, Y. Pan, G. Q. Zhou, T. L. Qu, H. Luo, and B. Zhang, in IEEE International Symposium on Inertial Sensors and Systems (2019).
[34]S. V. Joubert, M. Y. Shatalov, and C. E. Coetzee, J. Symbolic Comput. **61–62**, 116 (2014).